Special Issue (1), pp. 49-81, (2023)
DOI:10.21608/aujes.2023.178805.1110
Aswan University Journal of Environmental Studies (AUJES)
Special Issue: Impact of Climatic Change on Surface Water ecosystem and its biodiversity
Online ISSN: 2735-4237, Print ISSN: 2735-4229
Journal homepage: https://aujes.journals.ekb.eg/ E-mail: AUJES@aswu.edu.eg
Original research

Effect of green synthesized iron oxide nanoparticles on bacterial microbiome for clean up the crude oil

Abeer M. Salama[1], Emanne Rashad[2], Ahmed M. Elgarahy[1, 3*], Khalid Z. Elwakeel[1,4]

[1] *Environmental Science Department, Faculty of Science, Port-Said University, Port-Said, Egypt.*
[2] *Department of Environmental Sciences, Faculty of Science, Alexandria University, Alexandria, Egypt.*
[3] *Egyptian Propylene and Polypropylene Company (EPPC), Port-Said, Egypt.*
[4] *University of Jeddah, College of Science, Department of Chemistry, Jeddah, Saudi Arabia*

Received: 5/12/2022 Accepted: 1/1/2023

Supplementary Information

Effect of green synthesized iron oxide nanoparticles on bacterial microbiome for clean up the crude oil

Abeer M. Salama[1], Emanne Rashad[2], Ahmed M. Elgarahy[1,3]→, Khalid Z. Elwakeel[1,4]

[1] Environmental Science Department, Faculty of Science, Port-Said University, Port-Said, Egypt.

[2] Department of Environmental Sciences, Faculty of Science, Alexandria University, Alexandria, Egypt.

[3] Egyptian Propylene and Polypropylene Company (EPPC), Port-Said, Egypt.

[4] University of Jeddah, College of Science, Department of Chemistry, Jeddah, Saudi Arabia

→Corresponding author:
Environmental Science Department, Faculty of Science, Port-Said University, Port-Said, Egypt E-mail address: ahmedgarahy88@yahoo.com

Section 1. Characterization of GS-IONPs

For surface functional groups determination, Nicolet IS10 FTIR (Thermo Fisher Scientifc, Waltham, MA, USA) with an ATR addition lessened gross reflectance) was applied. The crystalline morphology of the prepared nanoparticles was employed using the Rigaku Miniflex diffractometer upon Cu-Kш rays. The angles applied in the XRD diffraction design was between 10° and 90°.The texture of GS-IONPs was investigated via differential light scattering by the DLS particle size analyzer NanoBrook 90Plus, Brookhaven Devices Company, Holtsville, NY, USA). For 25 °C-temperature magnetic induction trials expending a extreme 10 kOe magnetic arena, an exciting taster magnetometer, VSM (PMC MicroMag 3900, Lake Shore Cryotronics, Inc., Westerville, OH, USA,(was employed. A Nano Zeta Sizer (Nano-ZS Malvern Instruments Ltd., London, UK) was applied to enumerate the zeta potential of the formed nanoparticles at neutral pH and room temperature. The transmission electron microscope (TEM-2,2100HR, JEOL Ltd., Tokyo, Japan) was the instrument for ultra-high-accuracy description of ferric nanoparticles existed in the aqueous solution formerly the full deposition on carbon lattices surfaces.

Section 2. BOD, COD, and TOC measurements

For measurement of BOD, COD, and TOC in the inspected samples, the analytical procedures were employed as follow. The samples were filtered via cellulose acetate tissue filter (0.45-µm diameter, Whatman) and the residual BOD, and COD concentrations were systematically analyzed. The remaining BOD concentrations in the solution samples were established utilizing HI5421 Do/BOD/OUR/SOUR/Temperature Bench Meter, Hanna Instruments, USA. COD analysis typically includes applying the potassium dichromate oxidation procedure in the existence of sulfuric acid, and mercury sulfate to produce CO_2 and H_2O, the Vials were read in a spectrophotometer to define the results. The volume of potassium dichromate during the experiment was determined by comparing the volumes of ferrous ammonium sulfate taken in the blank and sample titrations. The quantity of potassium dichromate exploited in the reaction is equal the total amount of oxygen used to

degrade/oxidize the organic matter in dairy effluents (Federation and Association 2005). Finally, the total organic carbon (TOC) was measured using the Total Organic Carbon Analyzer (TOC-VWP, Shimadzu, Japan) by applying standard methods 5310B: high-temperature combustion technique. All tests were carried out in triplicate, and the averages were recorded.

Section 3. Results of GS-IONPs characterization

3.2.1. FTIR analysis

The FTIR spectra of E. Crassip extract and GS-IONPs are seen in Figure S1. For *E. crassipes* extract spectrum, some identification peaks were recorded in the range between 3180–1069 cm^{-1}. The band at 3180 cm^{-1} is attributed to O-H stretching vibrations of tannin molecule and absorption bands at 1641 cm^{-1} showed the presence of C=C. The C–C aromatic ring of the tannin molecule showed a peak at 1404 cm^{-1}, while the peak at 1069 cm^{-1} exhibited C-O-C vibrations.

The presence of magnetite nanoparticles is confirmed by an absorption band of about 587 cm^{-1}. Furthermore, the absorption bands at 1387 cm^{-1} revealed the capping agent's symmetric CH_3 vibration. The existence of a C-C aromatic ring from the tannin molecule (bio-reducing agent) was detected at 2148 cm^{-1} (Cardoso et al., 2014). Furthermore, the intensity of the peak observed at 3735 cm^{-1} is attributed to O-H stretching vibrations (Mohan Kumar et al., 2013).

3.2.2. X-ray diffraction analysis (XRD)

XRD pattern of GS-IONPs capped with *E. crassipes* extract is shown in Figure S2. Well-defined peaks were obtained at 30°, 35°, 43°, 53°, 51°, and 62.5° corresponding to (220), (311), (400), (422), (511), (440) orientation planes respectively. The diffraction peaks of GS-IONPs planes obtained are aligned with standard JCPDS file no. 85-14366 (Wang et al., 2011). This diffraction pattern indicated that the prepared NPs have very sharp peaks with ultrafine nature and high crystalline cubic spinel structure, which confirms the purity and good formation of the GS-IONPs (Azadi et al., 2018). Similar results were

obtained by other studies that described the synthesis of GS-IONPs using different plant extracts (Mahdavi et al., 2013; Senthilkumar et al., 2019; Yew et al., 2020).

3.2.3. The magnetic properties

The magnetization curve of GS-IONPs is shown in Figure S3. The magnetic properties of GS-IONPs are displayed in the symmetric hysteresis loop, and their saturation magnetization abilities are determined to be 53.65 emu g^{-1}. There was no hysteresis in the magnetization, and both remanence and coercivity were zero, indicating that these GS-IONPs are superparamagnetic.

3.2.4. Differential light scattering

The size of sorbent particles may be determined by Differential Light Scattering (DLS): Figure S4 shows the distribution of magnetite NPs particles size. GS-IONPs are nanometer-size with an average value of 15.21 nm which is slightly higher than the observed in the TEM pictures. This size difference may be attributed to that DLS calculates the hydrodynamic size of the as-prepared Fe_3O_4 NPs (Gittings and Saville, 1998).

3.2.5. Zeta potential

Results of zeta potential analysis of the prepared GS-IONPs are shown in Figure S5. The Zeta potential value of the prepared Fe_3O_4 NPs was -26 mV confirming its negative surface charge. According to Thakkar et al., NPs having a zeta potential larger than +25 mV or less than -25 mV have higher degrees of colloidal stability due to repulsive forces that prevent NPs from aggregating together (Thakkar et al., 2016); Large positive or negative zeta potential magnetic particles repel each other, resulting in a non-aggregated solution with good particle stability (Nallamuthu et al., 2013). The obtained result of prepared GS-IONPs indicated that the prepared GS-IONPs have a suitable dispersion capability in the aqueous medium.

Online ISSN: 2735-4237, Print: ISSN 2735-4229. https://aujes.journals.ekb.eg/

Table S1. $\bar{x}$ ± SD of microbial growth media absorbance at (620.0 nm), using different pH values and temperature degrees (°C).

Environmental parameter	Values	$\bar{x}$ ± SD of growth media absorbance at (620.0 nm)
pH	6.00	61.26±0.94
	7.00	73.93±1.15
	8.0	43.14±2.01
Temperature	27.0°C	42.21±2.01
	37.0°C	65.46±2.33
	47.0°C	34.07±1.56

.

Table S2. Kruskal-Wallis test for variation in absorbance pattern of bacterial growth media at 620 nm, using different pH values and temperature degrees (°C).

pH	**N**	**Median**	**Ave Rank**	**Z**
6	3	61.23	6.0	0. 77
7	3	73.12	6.8	1.42
8	3	43.00	2.2	-2.19
Overall	9	-	5.0	-
Chi square	5	-	-	-
DF	2	-	-	-
P value	0.082	-	-	-
Temperature	**N**	**Median**	**Ave Rank**	**Z**
27	3	42.12	5.0	0.00
37	3	65.25	8.0	2.32
47	3	34.65	2.0	-2.32
Overall	9	-	5.0	-
Chi square	7.20	-	-	-
DF	2	-	-	-

P value	0.027	-	-	-

Table S3. Average (±SD) of replicates tests of bacterial growth media absorbance at wavelength 620.0 nm using different concentrations of GS-IONPs (mg) at different time intervals.

Time (days)	GS-IONPs primary concentration (mg)						
	Control	**10.0**	**20.0**	**30.0**	**40.0**	**50.0**	**60.0**
3.0	36.33 ± 1.53	43.67± 1.53	56.33± 1.53	61.33± 1.15	85.67± 3.21	75.33± 3.51	69.00±3.61
6.0	54.00±2.00	72.00±3.00	82.33±0.58	125.33±0.58	146.33±1.53	133.67±3.21	130.33±1.53
9.0	86.33± 3.06	115.67± 3.51	127.67± 2.52	142.00± 2.65	170.67± 5.03	163.17± 1.53	154.00±2.65
12.0	104.00± 3.61	146.00± 3.61	176.33± 1.53	182.17± 2.02	207.33± 3.06	197.33± 2.08	185.67±3.21
15.0	95.67±2.08	142.00±10	172.67±3.79	177.33±2.52	191.33±1.53	182.33±2.52	176.00±20
18.0	82.67±2.52	135.67±2.08	158.33±5.03	163.33±4.73	188.00±2.65	107.67±1.53	102.00±3.00
21.0	76.17±1.04	114.33±3.51	150.00±2.00	164.67±3.21	173.33±4.16	99.67±1.53	83.33±4.16

Table S4. GLM test for variation in absorbance pattern of bacterial growth media at 620 nm, using different concentrations of GS-IONPs (mg) with different time intervals.

Growth media	Source	DF	Seq SS	Adj SS	Adj MS	F-value	P-value
Bacterial growth media + different concentrations of Fe_3O_4 NPs	Conc. of NPs (mg)	6	101065	101065	16844	54.86	0.000
	Time (days)	6	171064	171064	28511	92.87	0.000
	Error	134	41140	41140	307	-	-
	Total	156	313269	-	-	-	-

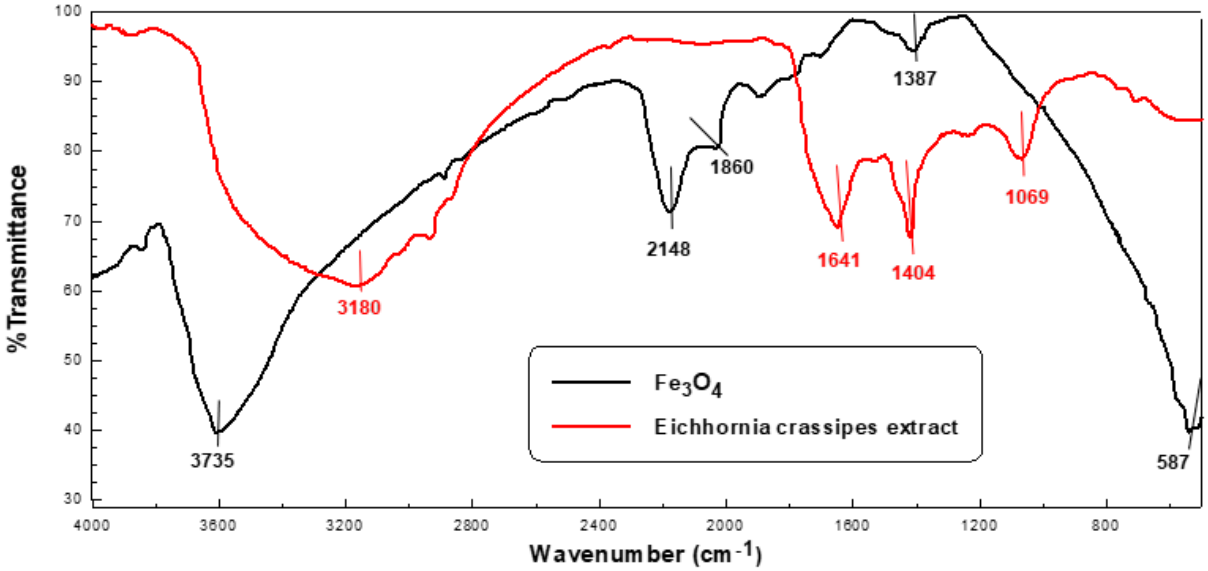

Figure S1. FTIR spectra of the synthesized GS-IONPs and *Eichhornia crassipes extract.*

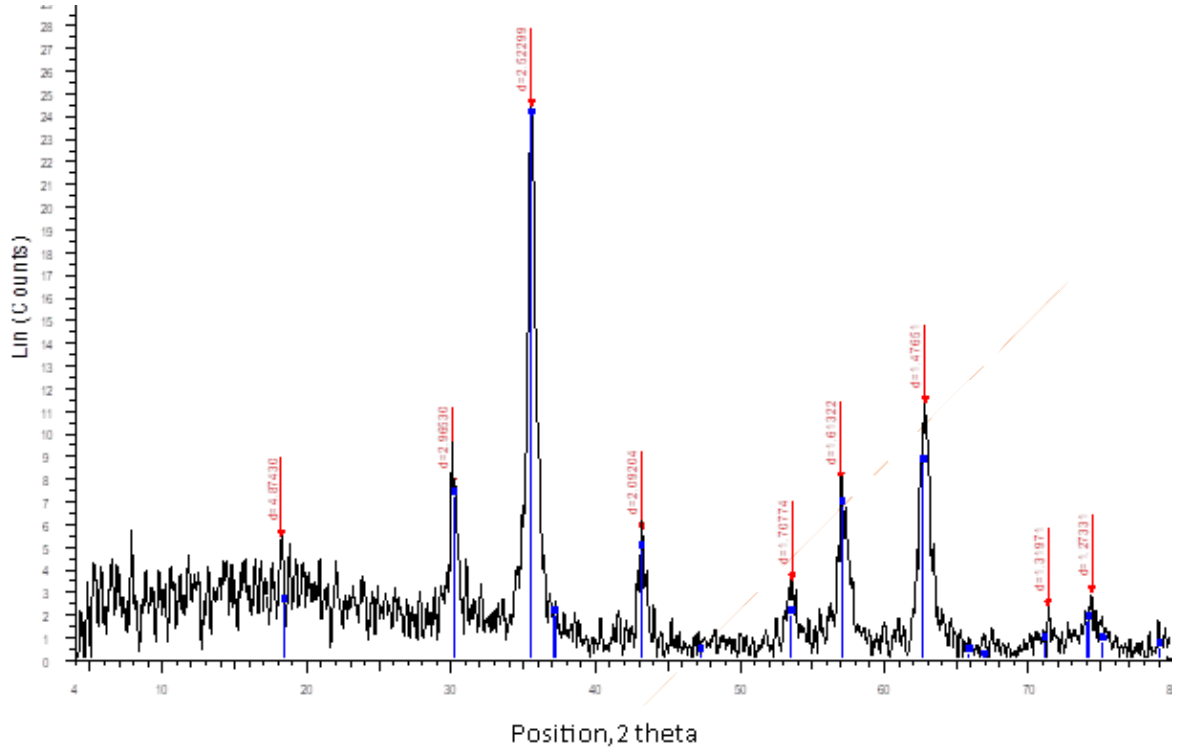

Figure S2. XRD pattern of Fe_3O_4 NPs reduced with *E. crassipes* extract. The signature peak intensity was defined by the JCPDS.

Online ISSN: 2735-4237, Print: ISSN 2735-4229. https://aujes.journals.ekb.eg/

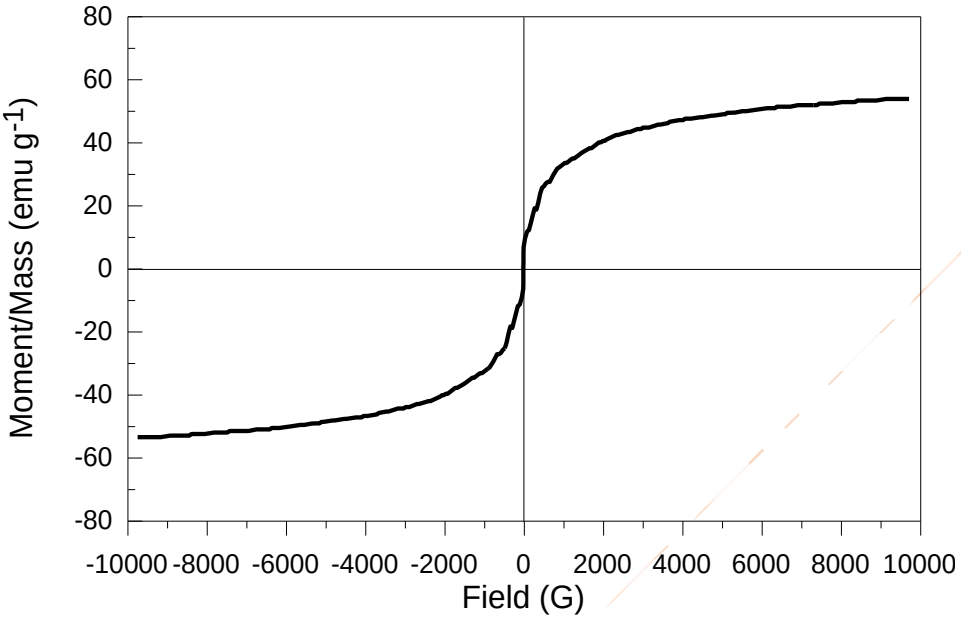

Figure S3. Magnetic properties: Vibrating sample magnetometry (VSM) curve of the synthesized GS-IONPs.

Online ISSN: 2735-4237, Print: ISSN 2735-4229. https://aujes.journals.ekb.eg/

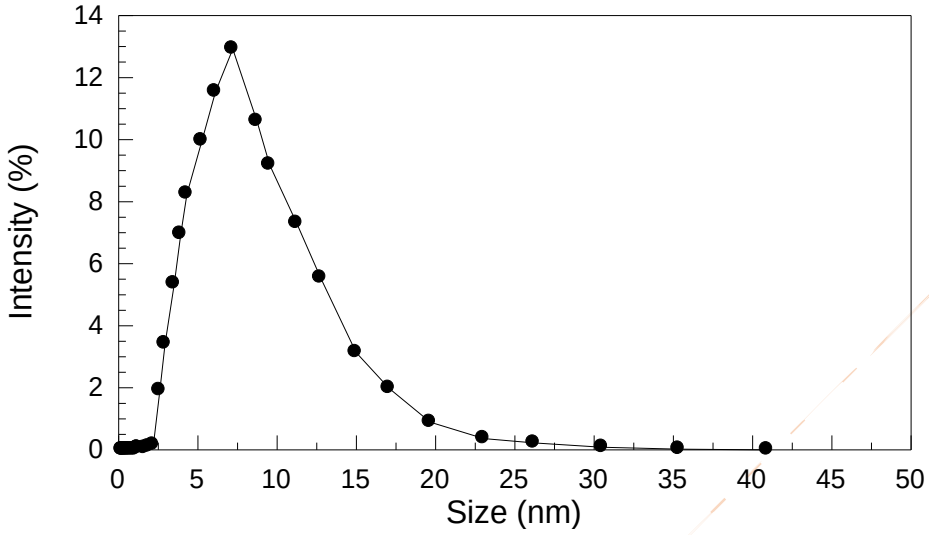

Figure S4. Particle size analysis – DLS (differential light scattering) of the synthesized GS-IONPs.

Online ISSN: 2735-4237, Print: ISSN 2735-4229. https://aujes.journals.ekb.eg/

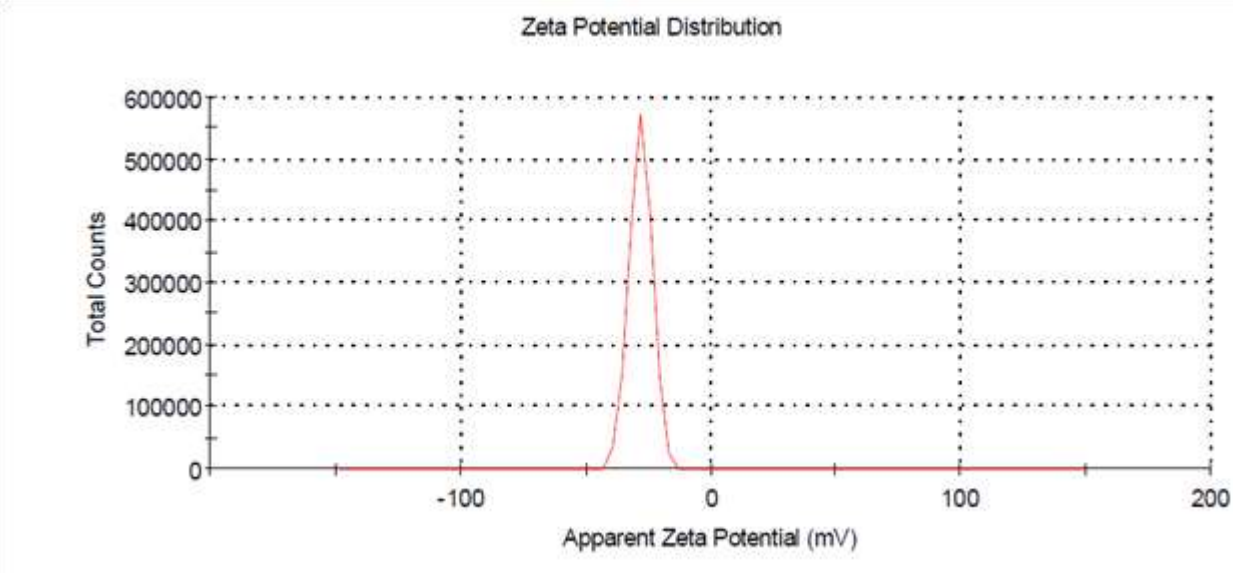

Figure S5. Zeta potential of GS-IONPs capped with *E. crassipes* extract.

References

Azadi, F., Karimi-Jashni, A. and Zerafat, M.M. (2018) Green synthesis and optimization of nano-magnetite using Persicaria bistorta root extract and its application for rosewater distillation wastewater treatment. Ecotoxicol. Environ. Saf. 165, 467-475.

Cardoso, S.F., Lopes, L.M.X. and Nascimento, I.R. (2014) Eichhornia crassipes: An advantageous source of shikimic acid. Revista Brasileira de Farmacognosia 24(4), 439-442.

Gittings, M.R. and Saville, D.A. (1998) The determination of hydrodynamic size and zeta potential from electrophoretic mobility and light scattering measurements. Colloids Surf. Physicochem. Eng. Aspects 141(1), 111-117.

Mahdavi, M., Namvar, F., Ahmad, M.B. and Mohamad, R. (2013) Green biosynthesis and characterization of magnetic iron oxide (Fe3O4) nanoparticles using seaweed (Sargassum muticum) aqueous extract. Molecules 18(5), 5954-5964.

Mohan Kumar, K., Mandal, B.K., Siva Kumar, K., Sreedhara Reddy, P. and Sreedhar, B. (2013) Biobased green method to synthesise palladium and iron nanoparticles using Terminalia chebula aqueous extract. Spectrochim. Acta A Mol. Biomol. Spectrosc. 102, 128-133.

Nallamuthu, I., Parthasarathi, A. and Khanum, F. (2013) Thymoquinone-loaded PLGA nanoparticles: antioxidant and anti-microbial properties. Int. Curr. Pharm. J. 2(12), 202-207.

Senthilkumar, P., Surendran, L., Sudhagar, B., DS, R.S.K. and Bupesh, G. (2019) Hydrothermal assisted Eichhornia crassipes mediated synthesis of magnetite nanoparticles (E-Fe3O4) and its antibiofilm activity. Mater. Res. Express 6(9), 095405.

Thakkar, S., Wanjale, S. and Panzade, P. (2016) Green synthesis of gold nanoparticles using Colchicum autumnale and its characterization. Int J Adv Res 4(4), 596-607.

Wang, Y.M., Cao, X., Liu, G.H., Hong, R.Y., Chen, Y.M., Chen, X.F., Li, H.Z., Xu, B. and Wei, D.G. (2011) Synthesis of Fe3O4 magnetic fluid used for magnetic resonance imaging and hyperthermia. J. Magn. Magn. Mater. 323(23), 2953-2959.

Yew, Y.P., Shameli, K., Miyake, M., Khairudin, N.B.B.A., Mohamad, S.E.B., Naiki, T. and Lee, K.X. (2020) Green biosynthesis of superparamagnetic magnetite Fe3O4 nanoparticles and biomedical applications in targeted anticancer drug delivery system: A review. Arab. J. Chem. 13(1), 2287-2308.